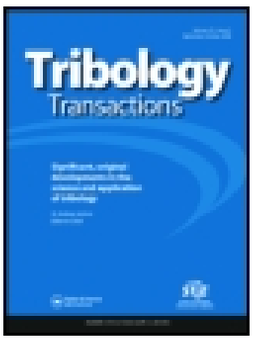

Tribology Transactions

ISSN: 1040-2004 (Print) 1547-397X (Online) Journal homepage: https://www.tandfonline.com/loi/utrb20

# Positron annihilation studies of subsurface zone created during friction in pure silver

Jerzy Dryzek & Krzysztof Siemek

**To cite this article:** Jerzy Dryzek & Krzysztof Siemek (2019): Positron annihilation studies of subsurface zone created during friction in pure silver, Tribology Transactions, DOI: 10.1080/10402004.2019.1600769

**To link to this article:** https://doi.org/10.1080/10402004.2019.1600769

Accepted author version posted online: 29 Mar 2019.

# Positron annihilation studies of subsurface zone created during friction in pure silver

Jerzy Dryzek[1], Krzysztof Siemek[2]

Institute of Nuclear Physics Polish Academy of Sciences, PL-31342 Krakow, Poland,

*Corresponding author: jerzy.dryzek@ifj.edu.pl

[1)]orcid.org/0000-0001-6594-123X

[2)]orcid.org/0000-0001-8345-1066

## Abstract

Positron lifetime research has been performed on well annealed pure silver samples after dry sliding, compression and sandblasting processes. These treatments affect the surface, but also have been shown significantly modify the region adjacent to the surface. The great number of dislocations decorated with monovacancies and jogs are observed, in the layer up to 110 μm beneath the surface. In the deeper layer, which extends to a depth of 300 μm, their concentration decreases gradually. Unlike other metals, the total depth of the subsurface zone induced by dry sliding is almost independent of the applied load. The significant increase in the positron lifetime has been observed in the layer 15 μm thick from the worn surface in the sample exposed to a long duration sliding test. Large clusters which consist of about twelve vacancies are observed in this layer. It can be a tribolayer that occurs as a result of dynamic recrystallization near the surface. This shows that conventional positron techniques can be effective tools in the investigation of defects in tribolayers, whose thickness is about several dozen micrometers. For a sample exposed to sandblasting the total depth of the subsurface zone is smaller, i.e. about 120 μm, however, the depth dependency of the positron lifetime is very similar to those obtained for dry sliding.

Keywords: Silver, Wear Mechanisms, Friction Test Methods



## 1. Introduction

Technological processes like machining, polishing, ion implantation, sandblasting, and sliding affect the surface of a product, however elastic and plastic deformation take place

as well below the surface. In the literature, the zone adjoining the surface with properties that are changed due to sliding or friction is called the work hardening zone because the increase of the hardness is the clearly apparent [1]. Moreover, some changes in physical properties extend beyond the work hardening zone and determine the boundaries of the so-called subsurface zone. Generation of the subsurface zone (SZ) is inherent in any surface treatment [2]. This paper addresses sliding contact when two surfaces slide against each other.

Generally, when two bodies are in sliding contact, the load at the surface is supported by asperities [3]. The asperities undergo elastic or plastic deformation as soon as they are in contact. High stress concentration in these regions can lead to damage and thus also crack initiation [4]. The asperity region is the source of dislocations that lead to stress concentration in the subsurface zone [5]. It is not excluded that the impacts between asperities cause propagation of deformation to large depths from the worn surfaces [6]. That is the deformation observed at depth of hundreds of micrometers from the surface [7]. The size of the asperities is on the order of a micrometer or less, however, the subsurface zone range is hundreds of micrometers. This zone contains crystalline defects generated during sliding which accompany the deformation, and their concentration decreases with increasing depth from the worn surface [8]. Usually, an exponential decrease with depth was observed, but other dependencies have also been observed [9]. The mechanism of SZ generation is still poorly understood. Nevertheless, the collection of new experimental data for various metals and alloys can help to get to know it.

The SZ is relevant to tribology but can affect electrical properties of conductors as well. Due to the skin effect, alternating electric current (AC) flows within a conductor near the surface. With the increasing frequency, the current becomes distributed closer to the surface. For instance, in silver at 1 MHz, current flows to a depth of about 63 μm from the surface. This depth coincides with the subsurface zone generated during sandblasting, which in copper is 140 - 800 μm as shown in recent studies [10]. Charges flow near the surface of wire or bar, but in this region, they can scatter at defects which may be created during the manufacture of wires or other devices. This effect can be even more pronounced for radio frequency (RF) cavities because the presence of surface and near surface defects reduces the electrical conductivity which affects, for instance, the Q factor which describes the energy loss relative to the stored energy of the resonator [11]. This can be enhanced if the resonator operates at low temperature since the main contribution to electrical

conductivity is scattering at crystalline defects. We, therefore, focused on the SZ in metals and alloys which are used for the construction of RF electronic devices. Silver is a electron conductor, widely used in electronics.

Experimental study of the SZ is not an easy task. One method involves microhardness measurement performed at a cross section of the worn sample. However, the microhardness is not sensitive enough to detect defects at the atomic scale. This is due to the large size of the indenter used, so one can only detect high defect concentrations using this method. Other methods such as XRD, SEM, or TEM (not HRTEM) are not sufficiently sensitive to point defects which are generated in great amount during dry sliding. Positron annihilation methods are suitable for these studies due to the large penetration depth of implanted positrons and their sensitivity to the different type of defects [12]. They can accurately detect the defect depth profile and the total range of the SZ as it was shown in many studies.

The aim of the paper is to recognize the type of defects and their depth distribution in pure silver exposed to dry sliding. From our previous research (see e.g., [6], [8],[9]), we noticed that in every metal exposed to dry slip other defects are generated and their depth distribution is also different. We suppose that in silver also unique distribution will be obtained. Conventional positron lifetime spectroscopy will be used to detect open volume defects at depths of one to hundreds of micrometers. The results for dry shifting will be compared with the results obtained by pressing and sandblasting to find some similarities. The possibility of dynamic recrystallization in this metal is also discussed. Then, the depth distribution of the defects will be measured for a silver sample exposed to a long duration of dry sliding test.

## 2. Experimental details

### *2.1. Positron lifetime measurements*

Positron lifetime spectroscopy is based on the fact that the time prior to annihilation which an implanted positron spends in condensed matter depends on the local electron density [12]. Briefly, higher electron density in the site where positron annihilates is correlated with lower lifetime value, see Eq. A2, Appendix I. The electron density is highest in the core region of an atom. However, the positively charged nuclei repel positrons into an interstitial region occupied by valence and conduction electrons. In this region the electron density is much lower, so annihilation in this region is the main contributor to positron

lifetime. The perfect crystalline lattice can be locally disturbed by defects, for instance, open volume defects like vacancies, vacancy clusters and/or dislocations. In such defects, the electron density is even lower than in the interstitial region. In addition, positively charged positron can be localized at these defects which causes a significant increase in positron lifetime value. For instance, the lifetime of a positron trapped at monovacancy is longer that in the bulk crystal by a factor of about 1.5. There are many articles about experimental measurements and theoretical calculations of positron lifetime values for bulk and defects in different materials because these values can be treated as fingerprints used to identify them [13].

The present work used conventional fast-fast coincidence positron lifetime spectrometer, based on the ORTEC units. As the detector two photomultiplayers XP2020Q coupled with $BaF_2$ scintillators were applied. The time resolution of the spectrometer was about 260 ps. The isotope $^{22}Na$ was used as the positron source. The isotope was enveloped into a 7 μm thick Kapton foil, with an activity of about 30 μCi. Positrons emitted from the source have sufficient energy ($E_{max}$=544 keV) to penetrate beyond the surface of a sample. For silver, the linear absorption coefficient for positrons is about 480 $cm^{-1}$, so about 63 % of positrons emitted from this source are stopped in the top 21 μm [14] (see computer code LYS-1 [15]). For this reason, this technique is not sensitive to surface defects and inhomogeneities adjacent to it. Mechanically mixed layers, oxides, and impurities, whose thickness is less than one micrometer, can be ignored in these considerations. In order to detect defects at such small depths, positrons must be slowed down to the energy of a dozen of keV, as is the case with variable energy positron beam technique [12], [16] . This technique is not used in these studies but has already been used successfully in the study of tribological problems, recently in niobium [17].

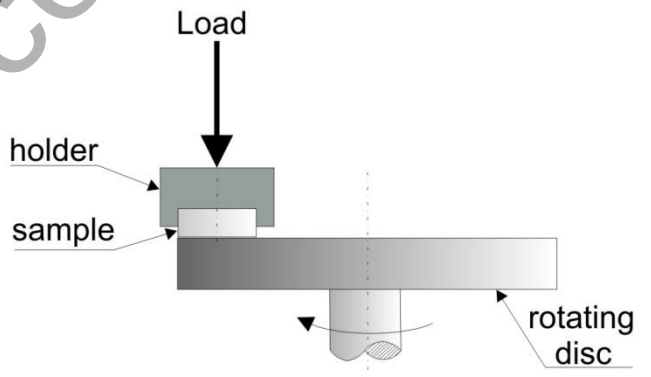


Fig. 1 The scheme of sample preparation in the tribotester.

### *2.2. Sample preparation*

Silver samples of 99.8% purity purchased from Goodfellow, used in our experiment had the shape of a disc with a diameter of 10 mm and a thickness of 2 mm. Initially, they were annealed in flowing $N_2$ gas at a temperature of 650$^{o}$C for 1 hr, and then slowly cooled to room temperature. Additionally, all samples were chemically polished by standard chemistry (1:1 volume mixture of $H_2O$:$HNO_3$) which etched away a layer of the surface about 50 μm thick. After this procedure, only residual defects are present in the samples. In fact, in the positron lifetime spectrum measured for virgin samples, only one lifetime component equal to 137±1 ps was resolved. This coincides with the value of 130 ps reported in the literature for positron annihilation in bulk silver [13].

After annealing and etching, a virgin sample of silver was mounted in the tribotester and the surface of the sample slid against a rotating disc at a load of 100 N for a duration of 1 minute. The scheme of the test is presented in Fig. 1. The rotating disc 50 mm in diameter was made of the high-speed steel (HS18 with hardness about 670 HV0.1). The speed of the disc relative to the surface of the sample was about 5 cm/s. The test was carried out in air for one minute. The average value of the friction coefficient and the specific wear rate, defined as the worn volume per unit sliding distance per unit of the load, were 0.29±0.02 and (2.46±0.08)×$10^{-14}$ $m^3N^{-1}m^{-1}$, respectively.

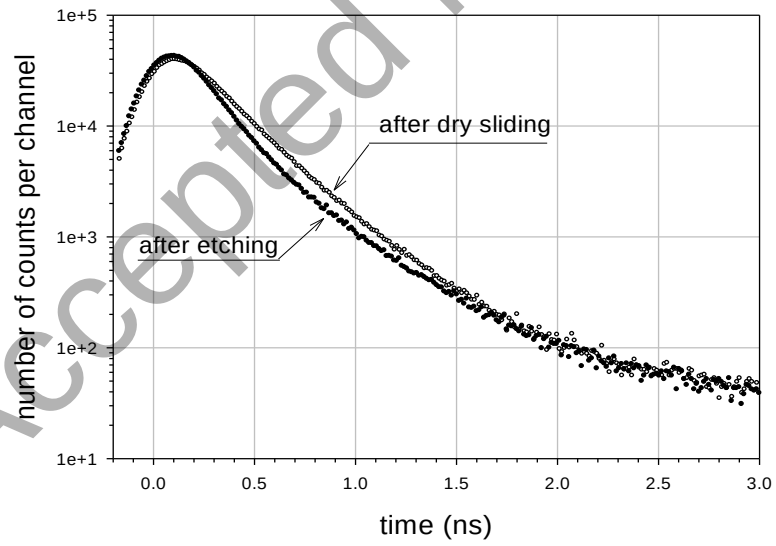


Fig. 2 The positron lifetime spectra measured for the silver sample after the dry sliding contact (open circles) and after etching of 300 μm thick layer from the worn surface (closed circles). The applied load was equal to100 N and for a duration of 1 minute.

In order to compare the results obtained for a dry slip test with a typical compression test, some of the virgin samples in the form of a disk were pressed in uniaxial pressing condition. The pressure was changed from 0 to 30 MPa to obtain the corresponding thickness reduction value. Then the effective true strain was calculated using the following equation [18]: $\varepsilon_{effect} = -\ln\left(1-\varepsilon/100\right)$, where $\varepsilon$ is the thickness reduction express in percent.

Our former results indicated similarity of the SZ induced during dry sliding with those obtained during sandblasting, for that reason so we want to know if in the case of silver this similarity also occurs. Two virgin samples were exposed to sandblasting using a Renfert Vario Basic Jet blaster. The abrasive material (Edelkorund containing 99.8% aluminum oxide) of particle size of 250 μm was used. The surfaces were blasted for 1 minute under the pressure of 1 bar with a distance of 10 mm between the sample and the perpendicularly directed nozzle. The estimated speed of particles hitting the surface is about 20 m/s. The nozzle diameter was 1 mm.

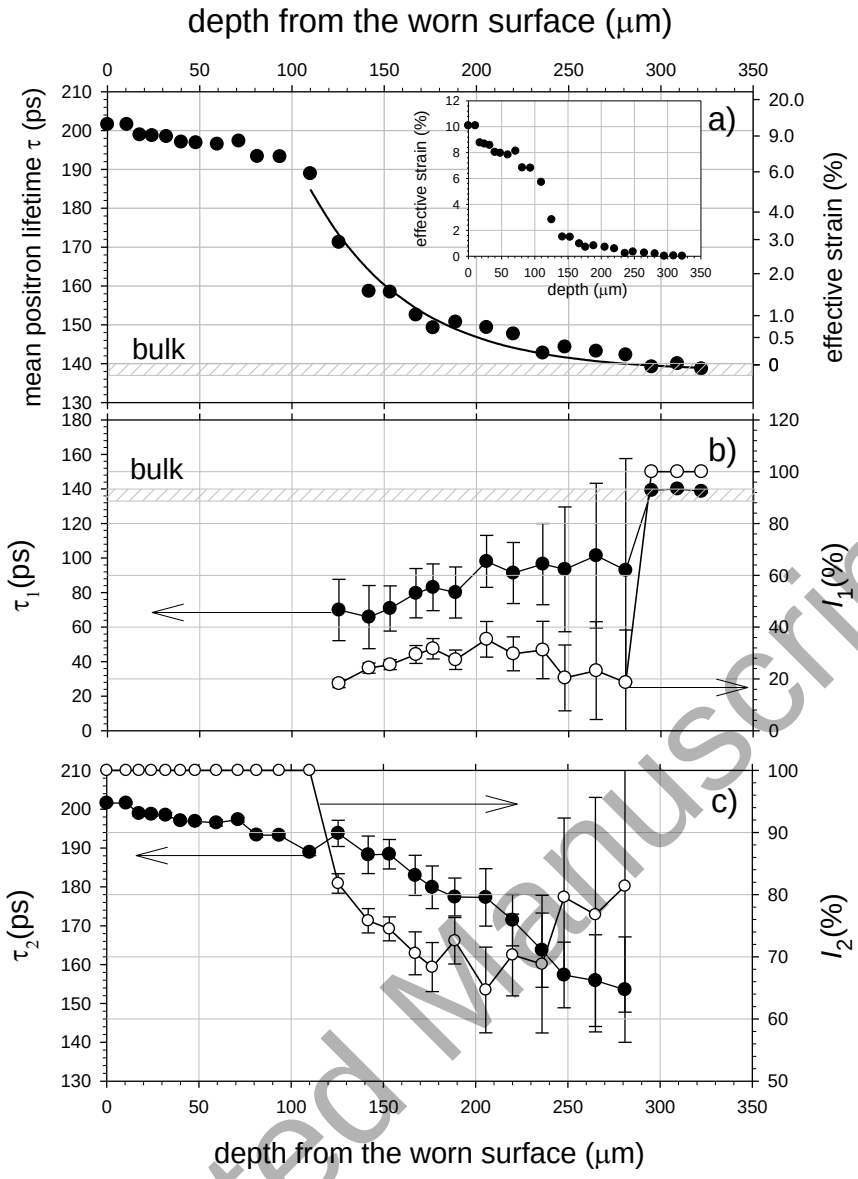


Fig. 3 The dependence of the positron mean lifetime values, calculated according to Eq. A7 on the depth from the worn surface of the pure silver exposed to dry sliding (a). The value of the first (closed circles, b) and the second (c) positron lifetime and their intensities (open circles) as a function of depth. The solid line represents the best fit of function $\bar{\tau} = \tau_0 \exp(-z/d) + \tau_{bulk}$ to the experimental points, see text. The hatched rectangle represents the bulk value of the positron lifetime in silver. In the inset, using the correlation function from Fig.4, the true strain as the depth function is shown.

The positron lifetime in the subsurface zone was measured using a sequenced etching, in the mixture of $H_2O$:$HNO_3$ mentioned above, a procedure as follows. The silver samples after dry sliding were etched to remove a layer about 10 μm thick from the worn surface, followed by measurement of the positron lifetime spectrum. The chemical etching does not

disturb the defect depth distribution in the remaining material. The thickness of the sample was measured using digital a micro-screw with accuracy ±1 μm. Fig. 2 shows positron lifetime spectra for the sample after dry sliding (open circles) and after sequentially etching of the 300 μm thick layer from the worn surface (closed circles). Significant changes in the spectra are clearly visible, their analyses are performed using LT computer code [19], [20], which allows extraction of the positron's life components, see Appendix I.

## 3. Results and discussion

### *3.1. Samples exposed to dry sliding*

The sequenced etching and measurements of positron lifetime spectra revealed their significant changes as it is seen in Fig. 2. One or two positron lifetime components depending on the depth were resolved in the obtained spectra, see Appendix I. Their values and intensities are gathered and depicted in Fig.3.

The mean positron lifetime value, calculated from Eq. A7, gradually decreases with the depth increase, as it is depicted in Fig. 3a. Up to the depth of about 110 μm this value slowly decreases from the value of 201 ps to 188 ps, then fast decrease to the value of about 150 ps at the depth of about 200 μm is observed. Beyond this depth, the long tail is observed which is extended to the depth of about 300 μm where the bulk value of the positron lifetime is reached. Thus the total depth of the damaged region induced in the sliding process is about 300 μm. This value corresponds with the similar values in other metals studied, e.g. Ref. [8].

A more detailed analysis of the obtained data indicates that in the depth range up to 110 μm, only a single lifetime component, which value from 200 to 190 ps, is resolved, as depicted in Fig. 3c (closed circles). Literature values of about 208 ps are attributed to monovacancies in the silver lattice [13] (see also Appendix II). We can, therefore, state that up to a depth of about 110 μm, this type of defect is generated during dry sliding. Values lower than 208 ps obtained at larger depth are also attributed to monovacancies, but those located near or at a dislocation, as reported for iron [21]. This value indicates the presence of dislocations with some vacancies located near or on the dislocation lines. Their concentration is so high that all positrons are located in such defects, hence the observed plateau.

At depths beyond 110 μm, two lifetime components in the spectra were resolved. The first one, $\tau_{1,}$ (Fig.3b, closed circles) is less than 130 ps, and the second one, $\tau_{2,}$ (Fig. 3c, closed circles) is between ca. 150 to 190 ps.

The fact that the $\tau_1$ value is smaller than the bulk value, is well explained by the two-state trapping model frequently use, see Appendix I, and Ref.[12]. According to this model, positrons can annihilate, both in a free and bound state trapped at a defect. In other words, a sample contains a bulk, non-defected region in which positrons can move freely and a defect that can trap them. The $\tau_1$ value is the reciprocal of the annihilation rate, the latter being the sum of the annihilation rate in the free state in bulk and the trapping rate at the defect, see Eq. A3. Because the trapping rate is proportional to the defect concentration then with its increase $\tau_1$ value decreases. We can conclude that the increase of the $\tau_1$ value, shown in Fig. 3 b indicates a reduction in defect concentration with increasing depth.

The value of the second lifetime component, $\tau_{2,}$ according to the two-state trapping model correspond directly to the positron lifetime trapped at a type of defect, in this case, dislocation with jog or monovacancy located near dislocation, Eq. A4. However, this value gradually decreases with depth increase, and its intensity also decreases from 80 to 65% (Fig. 3c, open circles). The latter also indicates that the dislocation concentration is decreasing with increasing depth, see Eq. A6. Simultaneously, the volume of the bulk region is increasing because the intensity of the first lifetime component, $\tau_{1,}$ is increasing from 20 to 38% (Fig. 3b, open circles). Similar behavior of lifetime components was observed in pure bismuth exposed to the dry sliding condition [22]. Above a depth of 280 μm a single lifetime component is resolved again, and its value tends toward the bulk value tagged in Fig. 3 a and b as a hatched rectangle. We argue that in the region up to 110 μm below the surface the concentration of defects induced by dry sliding is so high that the saturation of positron trapping takes place, it means each positron is trapped. Beyond this depth the mean positron lifetime decreases, this dependency can be recognized as the exponential decay function. The solid line in Fig. 3a represents the best fit of the function: $\bar{\tau} = \tau_0 \exp\left(-z/d\right) + \tau_{bulk}$, where $z$ is the depth from the worn surface, and $\tau_0$ and $d$ are adjustable parameters. This dependence is valid for $z$ >110 μm. The values of the parameters: of $\tau_0$=358(67) ps and $d$ = 54(4) μm, the latter characterize the gradient of defect concentration in this region, e.g. its low value indicates a large gradient and the opposite. The observed exponential decay of the mean positron lifetime with the depth

increase is a characteristic feature observed also in many metals, e.g. in magnesium [6], copper [8] or bismuth [22].

### *3.2. Samples exposed to compression*

The positron lifetime measurement reflects the local environment of the annihilation site at the atomic scale. However, it can also be associated with a macroscopic engineering parameter such as strain. This was clearly shown by many authors for a variety of metals and alloys, for instance for iron and its alloys exposed to the tensile stress the mean positron lifetime increases and saturate after thickness reduction of 10% [23]. Similarly, it was observed for nickel [24]. The results of positron annihilation for copper induced by normal loading of a spherical indenter were also compared with theoretical calculations of stress distribution and a good agreement was obtained [25], [26].

For obtaining a relationship between these two values, we performed measurements of the positron lifetime spectra for silver samples exposed to compression. In this measurement, two lifetime components were resolved. Fig. 4 shows the obtained values of the mean positron lifetime as a function effective true strain. The increase of the strain causes an increase of the positron lifetime, but above 10% values saturate at about 208 ps. This limits the applicability of positron lifetime measurements for determination of the true strain in the subsurface zone. Nevertheless, this dependency can be used for calibration of the true strain in the subsurface zone. First, the dependency is described using the following analytical function: $\bar{\tau} = \tau_{sat} + (\tau_{bulk} - \tau_{sat})\exp(-c\varepsilon)$, where $\varepsilon$ is the effective true strain in % and $c$ and $\tau_{sat}$ are the adjustable parameters in the fitting procedure. The solid line in Fig. 4 represents this function, which very well describes the obtained experimental dependence. the values of the adjustable parameters are as follows: $\tau_{sat}$=209.9(1.8) ps, $\tau_{bulk}$=139.6(2.4) ps and $c$=0.212(20). This can be used as a correlation function for the effective strain versus mean positron lifetime. In Fig.3a the vertical right axis represents the results of this correlation. We argue that at a depth of 110 μm the material exhibits defect density equivalent to a specimen compressively strained to about 6%, and then the deformation decreases with increasing depth, Fig. 3 a. It should be noted that the positron technique used in this work cannot be used to calculate strains exceeding 10%, and these are below 110 μm. A similar procedure has been successfully applied in the case of zirconium exposed to dry sliding, in this case an exponential decay of strain is found along with the increase in depth [9]. In the case of silver this dependency is more complex, see inset in Fig. 3a .

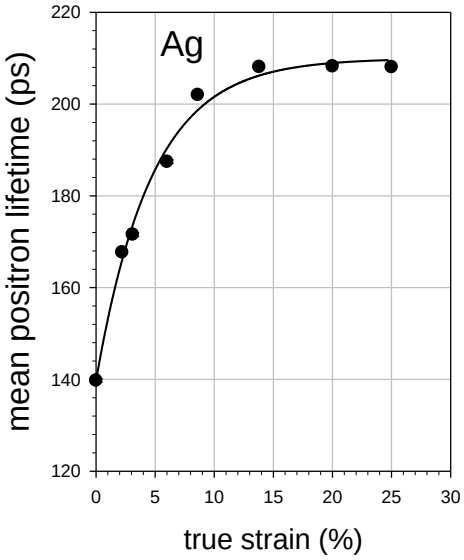


Fig. 4. The mean positron lifetime vs. the effective true strain of compressed well annealed pure silver. The solid line represents the best fit for the experimental points the following function: $\bar{\tau} = \tau_{sat} + (\tau_{bulk} - \tau_{sat})\exp(-c\varepsilon)$, where $\tau_{sat}$=209.9 ps, $\tau_{bulk}$=139.6 ps, and $c$=0.212.

### *3.3. Depth profile for other samples*

It is well known that the applied load affects the subsurface zone expansion. In silver, this is also observed and this is confirmed by Fig.5, where the mean positron lifetime value as the depth function for a different load is depicted. For loads of 50 N and lower, we observe gradual shrinking of the "plateau" adjoining the surface, which disappears for the 25 N load. Similar shapes of the depth profile of the mean positron lifetime were observed also for samples of titanium exposed to sliding performed in identical conditions [30]. However, for silver, the total depth of the subsurface zone is larger than in titanium where this value ranged from 130 to 250 μm. Additionally, the total depth of the subsurface zone is hardly affected by the applied load, where even for the lower load it is about 250 μm as shown in Fig. 5 and in Table 1 in the last row. For titanium we found that a simple sigmoidal formula describes the dependence of mean positron lifetime with depth as follows [30]:

$$\bar{\tau} = a + b\left[1 + erf\left(\frac{c - z}{\sqrt{2}\,d}\right)\right], \quad (1)$$

where $z$ is depth from the worn surface, *a, b, c,* and *d* are the adjusted parameters which can be obtained from the fitting procedure. The *c* parameter is the depth at which the

sigmoidal curve reaches the transition center and *b* is the transition height, here in ps unit. The parameter *d* characterizes the gradient of the decay in the transition region, and the *a* parameter corresponds to the bulk value. It turns out that this formula also well describes the results for silver, the solid and dashed lines in Fig. 5 represent the best fit of Eq. (1) to the experimental points. Table 1 shows all values of the adjustable parameters for the three dependencies.

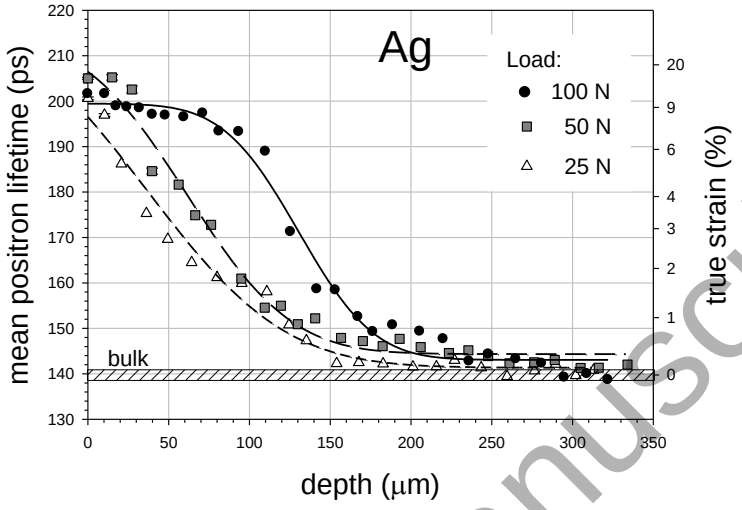


Fig. 5 The depth profiles of mean positron lifetime obtained for silver exposed to dry sliding at three values of the applied load. The duration of the tribotest was 1 minute for all samples. The solid, long dashed and short dashed lines represent the best fit of Eq. (1) to the experimental points.

**Table 1**. The values of the adjusted parameters in Eq. (1) used for the description of the obtained depth dependency of the mean positron lifetime depicted in Fig. 5, for three values of the applied load 25 N, 50 N, and 100 N. In the last row the total depth of the subsurface zone. This depth is defined as the depth where the bulk value of the mean positron lifetime is reached.

| | 100 N | 50 N | 25 N |
|---|---|---|---|
| *a* [ps] | 143(1.0) | 144(1.0) | 141(1.0) |
| *b* [ps] | 56(1.6) | 70(7.0) | 81(20) |
| *c* [μm] | 130(3.3) | 61(7.3) | 37(21) |
| *d* [μm] | 36(4.3) | 51(6.7) | 67(15) |
| total depth [μm] | 290 | 300 | 250 |

As expected, the *a* parameter remains almost constant, whereas that the *c* parameter decreases with

decreasing load, while the *d* parameter only slightly increases. The latter is opposite in the case of titanium as shown in Table 1 [30]. The explanation is simply that silver is an extremely soft and ductile metal in comparison to titanium, so that it can be deformed easily even at larger depth.

To find what affects the constitution of the SZ, let us compare the results for silver with those for the SZ in magnesium. [6], since this metal exhibits almost identical hardness to sliver but is not as ductile due to its hexagonal crystal structure. The face-centered cubic (fcc) structure of silver exhibits more sliding systems than the hexagonal structure (hex) in magnesium. The depth profiles of the mean positron lifetime value in magnesium shown in Fig. 1 in Ref. [6] and obtained in the almost identical condition the depth profile in Fig. 5 for silver, varies considerably. The latter has a plateau region and a long tail but in the first, there is only a continuous exponential decline of the positron lifetime value. The total depth of the SZ in magnesium depends on the applied load during tribotest, but in silver, this dependence is difficult to confirm, Table 1, last row. Therefore, we argue that the crystalline structure seems to be important in the constitution of the SZ. This is because defects generated during plastic deformation are associated with the crystal structure. Defects themselves directly are responsible for the dependencies like in Fig. 5. Another comparison, copper, like silver has fcc structure and only slightly higher hardness than silver, however, no plateau near the surface was observed in this metal [8]. But in both metals the stacking fault energy ($\gamma_{SFE}$) is different, It is known, that this affects also the mechanisms of plastic deformation, in metals with low values of $\gamma_{SFE}$ such as silver (~20 mJ/m$^2$) the dislocation dissociate and formation of stacking faults and twinning takes place, whereas in metals with high values of $\gamma_{SFE}$ such as copper (~80 mJ/m$^2$) slip deformation is preferred [27], [28]. In latter case, the dislocation movement causes creation of a large number of defects, including vacancies, they migrate and merge, forming clusters, as it is observed in copper [29]. In hex metals deformation begins by slip but can be accompanied by twinning because lack of sufficient slip systems. Vacancy clusters are also present in titanium, despite the observed plateau [30]. It should also be noted that the saturation of positron trapping requires a high level of defects and a high value of the positron's trapping efficiency. The latter depends on many factors including the electronic structure near or in a defect. According to Scheaffer [31], the trapping efficiency for vacancies in copper is about $3.8\times10^{16}$ 1/s and in silver about two times higher, $8.6\times10^{16}$ 1/s. This can also explain the saturation effect in silver compared to copper. Thus the

interaction between positrons and defects not related to sliding can affect the dependencies shown in Fig. 5. At this stage, it is still difficult to point out the major factor responsible for the expansion of the SZ.

### *3.4. Results for samples exposed to sandblasting*

Previous research indicated the similarity of the SZ induced by dry sliding and that induced by sandblasting, this was clearly visible in the case of pure magnesium [6]. Fig. 6 presents the obtained dependency of the mean positron lifetime as the function of depth from the surface. All features observed in Fig. 5 are also present in this dependency. First, a small plateau near the surface, then a fast decay, and finally a long tail similar to the results in Fig. 5 for the load of 50 N. The value of the mean positron lifetime at the surface in both cases are almost identical, of about 200 ps. Also in both cases, when the mean positron lifetime falls below 160 ps, a long tail appears in these dependencies, Fig. 3a, 5 and 6. However, the total depth of the subsurface zone is much smaller, about 120 μm. Presumably increasing pressure can increase this depth. It seems that also for silver the similarity of the subsurface zone for dry sliding and sandblasting was confirmed.

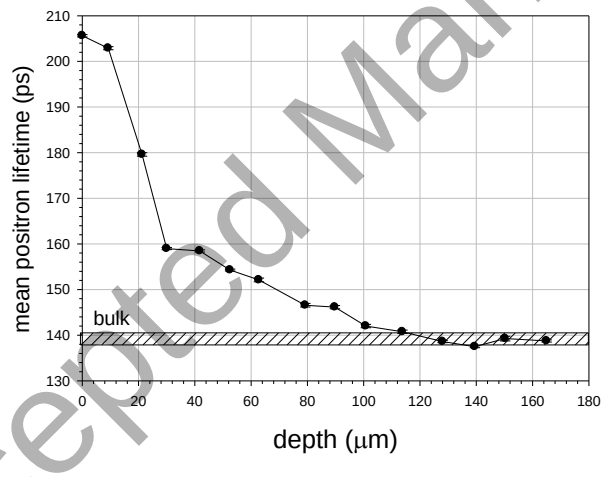


Fig. 6 The dependence of the mean positron lifetime as the function of depth for a sliver sample exposed to the sandblasting with alumina particles under the pressure of 1 bar.

### *3.5. Detection of a tribolayer*

Literature reports suggest that dynamic recrystallization can take place below the worn surface. This can lead to the formation of a few microns thick nanocrystalline layer just below the worn surface. Certainly, such a layer can have an impact on the wear and friction processes. Such a tribolayer in copper was first reported by Rigney et al. [32]. Others confirmed this effect for Ni-W alloy [33], [34], [35].

Dynamic recrystallization is characterized by nucleation and growth of new defect free grains that occurs during deformation rather than after deformation and during separate heat treatment, as in static recrystallization. Usually, it occurs during plastic deformation at high temperature. This process consists in the formation of new grains at the old grain boundaries. The nucleated new grains are free of defects, but the material continues to deform, causing an increase in dislocation density in the grain interior. This suppresses the grain growth or grains ceases to grow. Ultimately, dynamic recrystallization can result in very small grain size.

This process may take place when a critical deformation condition is reached in metals with low to moderate the stacking fault energy, such as copper or austenitic iron. This process has been observed in polycrystalline copper at 400$^{o}$C [36], which is close to the recrystallization temperature. We argue that silver, where the stacking fault energy is much smaller, is a good candidate for dynamic recrystallization which could accompany dry sliding. Additionally, the low value of recrystallization temperature of silver of about 60$^{o}$C [37] could promote this process. However, the results presented above do not suggest the existence of a layer of recrystallized grains near the worn surface in the silver samples. Such a layer would be manifested by a reduction of the mean positron lifetime, if the grains were defects free, or significant increase of the mean positron lifetime, because a generation of new grain boundaries, that contain many open volume defects.

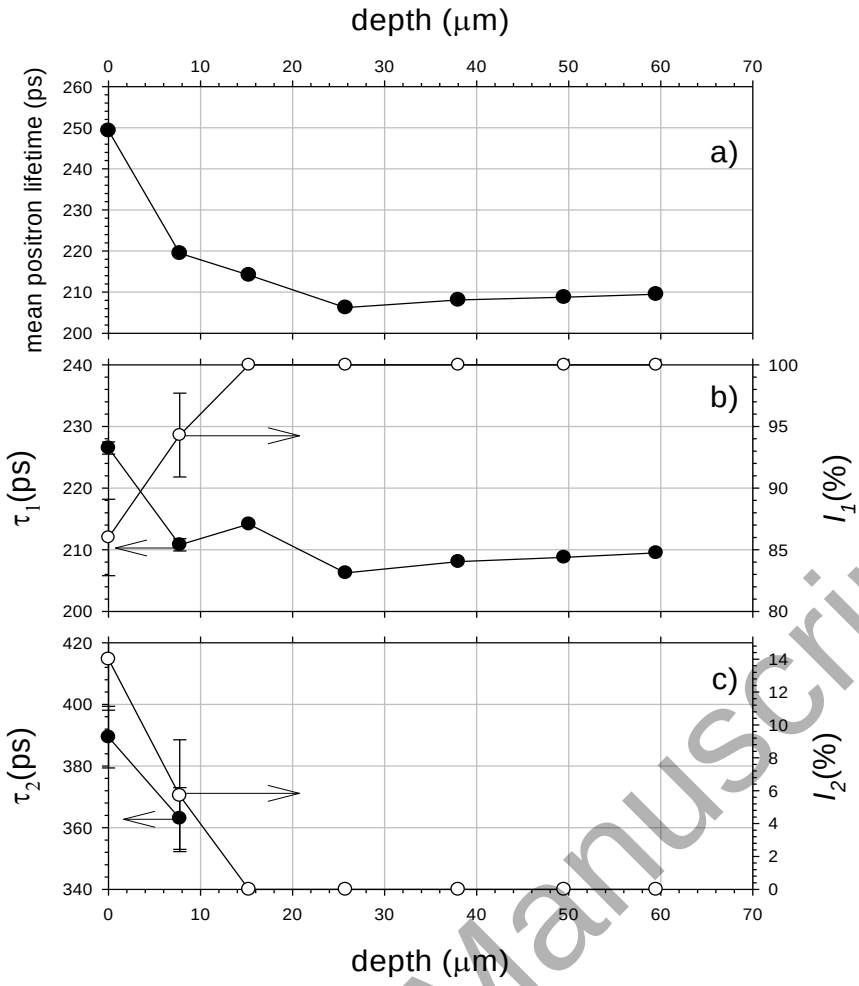


Fig. 7 The variation of the mean positron lifetime value (a) as a function of the depth for the silver sample exposed to dry sliding test with the load of 100 N during a much longer time, i.e., 45 min. Corresponding values of the first (closed circles, b) and the second (c) positron lifetime and their intensities (open circles) as a function of depth.

Previous authors observed a recrystallized layer after a long duration of the sliding test, on the order of 1 hour. However, the sliding duration in our tests was only 1 minute. In order to reveal the tribolayer in sliver a much longer sliding test was performed. We observed that after 10 minutes of sliding at a load of 100 N, the positron lifetime increases to about 248 ps, and after 45 minutes of sliding two lifetime components occur. The first one is equal to 226±4.0 ps, and the second 389±20 ps with an intensity of about 14 % and the mean positron lifetime value increases to 249 ps. The results for this case as the depth function are shown in Fig.7. It should be noted that in this case, the thickness of the etched layer was about 8 μm. The occurrence of such a long lifetime component indicates the presence of large vacancy clusters. According to the *ab initio* calculations presented in Appendix II and Fig. 8, the clusters consist of about twelve vacancies. Such defects can be

present at grain boundaries. The fact that they are observed by positrons indicates the small size of the grains. The value of the first lifetime component is much higher than the bulk value, so a large number of dislocations are present as well. This can indicate the existence of a new layer full of dislocations and vacancy clusters, which were not induced in the previous test.

Surface etching similar to the previous sample was performed to probe the depth of this layer. The second lifetime component of 363 ps with the intensity of 6 % is still present at the depth of about 8 μm, and disappears at depths more than 15 μm, Fig. 7 c. At greater depth only a single lifetime component of 207 ps is present, corresponding to the results in Fig. 3a and Fig 5.

In Fig. 7a the mean positron lifetime as the depth function is depicted. The significant increase of the mean positron lifetime near the worn surface is apparent. This layer about 15 μm thick is located above the zone which contains a great number of dislocations, as proposed above. This suggests that this is the layer with fine grains, resulting preassembly from the dynamic recrystallization. However, one cannot exclude the possibility that this layer originates from the compression of mixed debris. Therefore, this experiment for the first time demonstrates the use of positron annihilation to reveal the existence of such a tribolayer. Its existence was confirmed in our further measurements in pure iron, copper, stainless steel and silver alloy [46].

## 4. Conclusions

The defect profile in the subsurface zone of pure silver was detected by sequential etching of the surface layer exposed to dry sliding. The SZ contains monovacancies up to the depth of 110 μm, beyond vacancies associated with dislocations and undamaged, bulk region are present. Total depth of the SZ is more than 300 μm and it is hardly affected by the applied load. A similarity of the measured depth profiles of positron lifetime obtained in dry sliding and sandblasting was observed. Long duration of dry sliding causes the occurrence of a layer adjoining the worn surface which consists of a large number of dislocations and big vacancy clusters. Its thickness is about 15 μm and can result from the dynamic recrystallization. This work demonstrates the emergence of the tribolayer in silver detected by positron lifetime spectroscopy.

**Appendix I**

In the positron lifetime spectroscopy for defects in solids, the positron lifetime spectra are fitted, after source and background corrections, to a sum of exponentially decaying components as follows:

$$-\frac{dn(t)}{dt}=\left[\frac{I_1}{\tau_1}\exp\left(-\frac{t}{\tau_1}\right)+\frac{I_2}{\tau_2}\exp\left(-\frac{t}{\tau_2}\right)+...\right]\otimes R(t)+Bg \quad , \text{A1}$$

where $\tau_i$ and $I_i$ are the lifetime values and their relative intensities, respectively. $Bg$ represents a constant background. The $R(t)$ is the Gaussian function. A number of components in the sum depends on a number of states in which annihilation takes place Due to difficulties of statistical origin, it is usually possible to use only two components, but more components can be use as well. Computer codes, for instance, LT code [19], [20], allow to extract the intensities $I_i$ and lifetime values $\tau_i$ accurately.

The positron lifetime is associated with the annihilation rate $\lambda$ and positron $\Psi_+$ and electrons wave functions $\psi_I$ as follows [12]:

$$\lambda=\frac{1}{\tau}=\pi r_e^2 c\int_\Omega d^3\vec{r}\left|\Psi_+(\vec{r})\right|^2 g(\vec{r},\vec{r})\left(\sum_j\left|\psi_j(\vec{r})\right|^2\right), \text{A2}$$

where $g$ is the enhancement factor which takes into account many body interactions between electrons and positron, and $r_e$=2.818 fm is the classical electron radius and c speed of light. This equation shows that the positron lifetime depends strictly on the electron density in the annihilation site. In metals in perfect crystalline lattice single lifetime is observed, because a positron occupies only the interstitial site. This value we call as the bulk lifetime: $\tau_b$ and can be calculated from Eq. A2, but in practice, it requires the use of advanced calculation methods, see Appendix II.

The decomposition of the positron lifetime spectrum is explained by the trapping model proposed by Bertolaccini et al. [38], and Brandt [39]. This gives the rate equations for the positrons annihilating in bulk states when positrons are randomly walking and in localized states when they are trapped. If there is only one type of defect, for instance, monovacancy, in the sample, the solution to the kinetic equations gives two lifetime components, the first is as follows:

$$\tau_1=\frac{\tau_b}{1+\tau_b\kappa_v}. \text{A3}$$

$\kappa_v=\mu_v C_v$, is the positron trapping rate, where $C_v$ is the vacancy concentration and $\mu_v$ is the trapping rate coefficient. The value of the second component is equal to:

$$\tau_2=\tau_v \text{ , A4}$$

and correspond to the positron lifetime trapped at vacancy. The intensity of the first lifetime is equal to:

$$I_1=\frac{\tau_2-\tau_b}{\tau_2-\tau_b+\tau_2\tau_b\kappa_v} \text{ , A5}$$

and the intensity of the second component equals to:

$$I_2=1-I_1=\frac{\tau_2\tau_b\kappa_v}{\tau_2-\tau_b+\tau_2\tau_b\kappa_v} \text{ . A6}$$

We can notice that the intensities depend on the vacancy concentration $C_v$. The useful value is the mean positron lifetime defined as follows:

$$\bar{\tau}=\tau_1 I_1+\tau_2 I_2 \text{ . A7}$$

This value can be calculated directly from the experimental points as the first moment of the spectrum about the time zero or from the extracted lifetimes and their relative intensities. In the presented above model is so-called two-state trapping model, the mean positron lifetime is equal to.

$$\bar{\tau}=\tau_b\frac{1+\kappa_v\,\tau_2}{1+\kappa_v\,\tau_b} \text{ , A8}$$

and its value increases from $\tau_b$ to $\tau_2$ as the vacancy concentration increases. In the literature one can find appropriate relation for more sophisticated models, which take into account not only more defect types which can localize positrons but also diffusion of thermalized positrons to the crystalline grain boundaries [12], [37].

**Appendix II**

It is well known that the value of positron lifetime in vacancy clusters depends on their size, because lowering the electron density inside, Eq. A2. This link can be obtained using *ab initio* theoretical calculations using the PAW formalism as implemented in ABINIT code [40], [41]. For Ag numerical calculations were carried out using this code and a similar method as for Zr, see Ref. [9]. The proper potential for Ag was chosen from the available in pseudopotential repository [42], [43] and other parameters from Ref. [44] and [45] and In Fig. 8 the dependency of the positron lifetime as a function of the number of vacancies in a cluster is depicted. This dependency corresponds with the dependencies obtained by other authors for other metals.

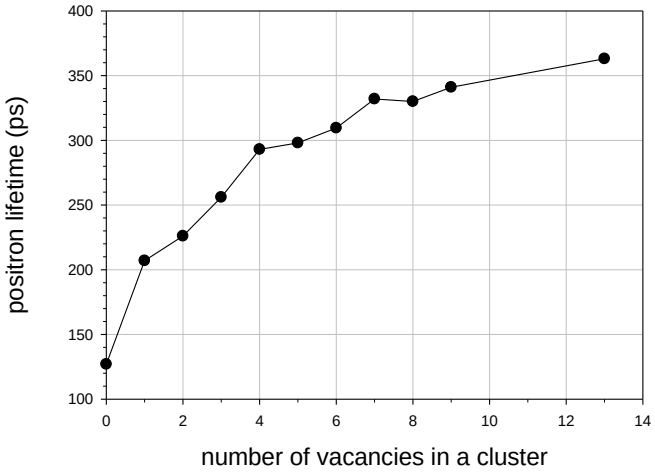


Fig. 8 Positron lifetime as a function of the number of vacancies in a cluster in Ag calculated using ABINIT code.

## 5. References

[1] Zum Gahr, K.-H. (1987), "Microstructure and Wear of Materials," Elsevier, Amsterdam, Oxford, New York, Tokyo, ISBN 0-444-42754-6.

[2] Horodek, P., Dryzek, J., Wróbel, M. (2012), "Positron Annihilation Study of Defects Induced by Various Cutting Methods in Stainless Steel Grade 304," Tribology Letters, **45**, pp 341-347.

[3] Bowden, F.P., Tabor, D. (1950), "Friction and Lubrication of Solids," Oxford University Press, ISBN 0 19 850777 1.

[4] Carbone, G., Bottiglione, F. (2008), "Asperity Contact Theories: Do They Predict Linearity Between Contact Area and Load?," Journal of the Mechanics and Physics of Solids, **56** (8), pp 2555– 2572.

[5] Wert, J.J. (1989), "The Role of Microstructure in Subsurface Damage Induced by Sliding Contact," Key Engineering Materials, **33,** pp. 101-134.

[6] Dryzek, J., Dryzek, E., Suzuki, T., Yu, R. (2005), "Subsurface Zone in Pure Magnesium Studied by Positron Lifetime Spectroscopy," Tribology Letters, **20**, pp 91-97.

[7] Kennedy, F.E. Jr. (1989), "Plastic Analysis of Near-Surface Zones in Sliding Contacts of Metals," Key Engineering Materials, **33**, pp 35-48.

[8] Dryzek, J., Dryzek, E., Stegemann, T., Cleff, B. (1997), "Positron Annihilation Studies of Subsurface Zones in Copper," Tribology Letters, **3**, pp 269–275.

[9] Dryzek J., Siemek K. (2016), "Formation of Subsurface Zone Induced by Sliding Wear in Zirconium Studied by Positron Lifetime Spectroscopy," Tribology Letters, **64**, pp 15-25.

[10] Horodek P., Siemek K., Dryzek J., Wróbel M. (2017), "Positron Annihilation and Complementary Studies of Copper Sandblasted at Different Pressures," Material **10** pp 1343-1358.

[11] Visentin B., Gasser Y., Charrier J.P. (2006), "First Results on Fast Baking," Physica C, **441**, pp 66-69.

[12] Puska M.J., Nieminen R. M. (1994), "Theory of positrons in solids and on solid surfaces," Rev. Mod. Phys. 66, pp 841-897.

[13] Robles, J.M.C., Ogando, E., Plazaola, F.J. (2007), "Positron Lifetime Calculation for the Elements of the Periodic Table," Journal of Physics: Condensed Matter, **19**, pp176222-20.

[14] Dryzek J., Siemek K. (2013), "The Multi-Scattering Model for Calculations of Positron Spatial Distribution in the Multilayer Stacks, Useful for Conventional Positron Measurements," Journal of Applied Physics, **114,** pp 074904-11.

[15] Dryzek, J, Siemek K, (2013) LYS-1 code available at: https://www.ifj.edu.pl/private/jdryzek/page_r22.html (accessed August 20, 2015).

[16] Van Veen A., Schut H., Mijnarends P.E. (2000) in "Positron beams and their applications," Coleman P.G. (ed.) World Scientific, Singapore, ISBN 981-02-3394-9

[17] Dryzek, J. ,Horodek, P. (2017), "Positron annihilation studies of the near-surface regions of niobium before and after wear treatment," Tribology Letters, **65**, pp 117-125.

[18] Alting, L. (1994), "Manufacturing Engineering Processes," Marcel Dekker Inc., New York, ISBN 0824791290 9780824791292.

[19] Kansy, J. (1996), "Microcomputer Program for Analysis of Positron Annihilation Lifetime Spectra," Nuclear Instruments and Methods in Physical Research, A **374**, pp 235-244.

[20] Kansy J. LT programs. http://prac.us.edu.pl/~kansy/index.php?id=lt10, Accessed date: 16 November 2010.

[21] Kamimura, Y., Tsutsumi, T., Kuramoto, E. (1995), "Calculations of Positron Lifetimes in a Jog and Vacancies on an Edge-Dislocation Line in Fe," Physical Review, B **52**, pp 879-889.

[22] Dryzek, J. (2010)," Positron studies of subsurface zone created in sliding wear in bismuth ," Tribol. Lett. 40, pp 175–180.

[23] Somieski, B., Krause-Rehberg, R. (1995), "Application of the positron lifetime spectroscopy as a method of non-destructive testing," Mater. Sci. Forum 175–178, pp 989–992.

[24] Dlubek G., Brümmer O., Hensel E. (1976), “Positron annihilation investigation for an estimation of the dislocation density and vacancy concentration of plastically deformed polycrystalline Ni of different purity,” Phys. Stat. Sol. (a) 34, pp 737-746.

[25] Dryzek J., Dryzek E. (2003), "Aplication of positron annihilation studies of the subsurface zones beneath the surface exposed to the normal loading", Tribol. Lett. 15 , 309-317.

[26] Dryzek J., Nojiri S., Fujinami M. (2014), "The positron microscopy studies of the wear tracks on the copper surface ,”Tribol. Lett. 56 ,pp 101-106.

[27] Hirth, J.P., Lothe, J. (1992), "Theory of Dislocations," Krieger Publishing Co., Malabar, Florida, Second Ed., ISBN-13: 978-0894646171.

[28] Murr, L.E. (1975), “Interfacial Phenomena in Metals and Alloys,” Addison-Wesley, ISBN 13: 9780201048858

[29] Dryzek J., Polak A. (1999), "Subsurface Zone Studied by Positron Lifetime Measurements,"Tribol. Lett. , 7, pp 57-60.

[30] Dryzek, J., Wróbel, M. (2014), "Positron studies of subsurface zone in titanium created in sliding wear," Tribol. Lett., 55 , pp 413-419.

[31] Schaefer, H.-E. (1987), "Investigation of Thermal Equilibrium Vacancies in Metals by Positron Annihilation. Physica Stauts Solidi (a) **102**, 47-65 (1987).

[32] Rigney, D.A., Chen, L.H., Naylor, M.G.S., Rosenfield, A.R. (1984), "Wear Processes in Sliding Systems," Wear, **100**, pp 195-219.

[33] Emge, A., Karthikeyan, S., Rigney, D.A. (2009), “The Effects of Sliding Velocity and Sliding Time on Nanocrystalline Tribolayer Development and Properties in Copper,” Wear, **267**, pp 562-567.

[34] Yao, B., Han, Z., Lu, K. (2012), ”Correlation Between Wear Resistance and Subsurface Recrystallization Structure in Copper,” Wear **294–295**, pp 438–445.

[35]. Timothy, J. R, Schuh, C.A. (2010), “Sliding Wear of Nanocrystalline Ni–W: Structural Evolution and the Apparent Breakdown of Archard Scaling,” Acta Materiala, **58**, pp 4137–4184.

[36] Ardakani, M.G., Humphreys, F.J. (1992), “Recrystallization’92”, eds. Fuentes and Gil Sevillano, Transaction Technical Publications, 213.

[37] Dryzek, J., Wróbel, M., Dryzek, E. (2016), “Recrystallization in Severely Deformed Ag, Au and Fe Studied by Positron Annihilation and XRD Method,” Physica Status Solidi B, **253**, pp 2031-2042.

[38] Bertolaccini, M., Bisi A., Gambarini G., Zappa L, (1971), " Positron states in ionic media," J. Phys. C: Solid State Phys. 4, pp 734-745.

[39] Brandt, W., (1974), " Positron dynamics in solids," Appl. Phys. 5, 1-23.

[40] Blöchl P.E (1994), "Projector augmented-wave method," Physical Review B, **50**, pp 17953-17979.

[41] ABINIT code available at: https/:/www.abinit.org (accessed 2004).

[42] Kevin F. Garrity,K.F., Bennett, J. W., Rabe K. M., Vanderbilt D. available at: https://www.physics.rutgers.edu/gbrv/ (accessed September 23, 2015).

[43] Garrity, K.F., Bennett, J.W., Rabe, K.M., Vanderbilt, D. (2014), "Pseudopotentials for High-Throughput DFT Calculations," Computational Material Science, **81**, pp 446–452.

[44] Vanderbilt, D. (1990), "Soft Self-Consistent Pseudopotentials in a Generalized Eigenvalue Formalism," Physical Review B, **4**, pp 7892-7895.

[45] Sterne, P.A., Keiser, J.H. (1991), "First-Principles Calculation of Positron Lifetimes in Solids," Physical Review B, **43**, pp 13892-13898.

[46] Dryzek, J. (2018), "Detection of tribolayer in different metals using positron lifetime spectroscopy," Tribol. Int. 131, pp 268-276.